The solar chromospheric Ca and Mg indices from Aura OMI

Matthew DeLand[1] and Sergey Marchenko[1]

Received 21 November 2012; revised 22 February 2013; accepted 3 March 2013; published 30 April 2013.

[1] Direct observations of long-term variations in solar UV irradiance from satellites, although important for monitoring the energetic forcing of the Earth's atmosphere, is challenging because of the difficulty of accurately tracking instrument response changes. Proxy indexes based on core-to-wing ratios of solar Fraunhofer lines, such as the Mg II feature at 280 nm, can minimize the impact of both time- and wavelength-dependent instrument changes to better monitor solar UV activity. Here we present new data sets from the Ozone Monitoring Instrument (OMI) on the Aura satellite, which began operations in late 2004. The high quality of OMI irradiance measurements allows us to construct daily indexes for the Mg II, Ca II K (393.4 nm), Ca II H (396.8 nm), and Mg I (285.2 nm) lines. The OMI Ca II K index is well correlated with the Mg II index measured by multiple instruments, as well as the ground-based National Solar Observatory (NSO) Ca II K 1.0 Å index data derived from Integrated Sunlight Spectrometer measurements. OMI Ca II K data can be used to evaluate anomalous short-term features in the NSO data set. The OMI solar data products represent a valuable addition to current data sets.

Citation: DeLand, M., and S. Marchenko (2013), The solar chromospheric Ca and Mg indices from Aura OMI, *J. Geophys. Res. Atmos.*, *118*, 3415–3423, doi:10.1002/jgrd.50310.

1. Introduction

[2] Solar variability is a key driver in the long-term behavior of atmospheric composition and global climate. The direct influence of solar irradiance is experienced through the photolysis of many constituents in the middle and upper atmosphere, and heating due to absorption of solar radiation [*Brasseur and Solomon*, 2005]. Solar observations at the Ca II K (393.4 nm) and Ca II H (396.8 nm) features are valuable indicators of solar UV activity and variability. These wavelengths penetrate through the Earth's atmosphere to the surface, which has allowed photographic records of the Sun at these wavelengths to be compiled for more than 100 years [*Foukal et al.*, 2009]. While the broad solar Ca II lines appear in absorption, the line cores show emission reversals arising from the solar chromosphere. Quantitative measures that can be determined from such observations include integrated parameters such as the 1 Å emission index [*White and Livingston*, 1981; *Keil and Worden*, 1984; *Livingston et al.*, 2010], as well as measures such as plage area that require image classification and interpretation [e.g., *Ermolli et al.*, 2009; *Tlatov et al.*, 2009; *Bertello et al.*, 2010]. These quantities have been used as proxies for solar activity at shorter UV wavelengths that do not penetrate the terrestrial atmosphere [e.g., *Lean et al.*, 1997; *Morrill et al.*, 2011b]. Ground-based measurements of Ca II behavior are constrained by local weather conditions and the challenges of maintaining a long-term observing program with a stable instrument configuration.

[3] Satellite measurements of solar irradiance provide the opportunity to observe the entire solar UV spectrum on a daily basis. Regular measurements of solar spectral UV irradiance began with the Nimbus-7 Solar Backscatter Ultraviolet (SBUV) spectrometer instrument in November 1978 [*DeLand and Cebula*, 2001] and continued with the Solar Mesosphere Explorer instrument [*Rottman*, 1988]. Other significant solar UV irradiance data sets acquired since that time include Upper Atmosphere Research Satellite (UARS) Solar Ultraviolet Spectral Irradiance Monitor (SUSIM) [*Floyd et al.*, 2003], UARS Solar Stellar Irradiance Comparison Experiment (SOLSTICE) [*Rottman et al.*, 2001], NOAA-9 SBUV model 2 (SBUV/2) [*DeLand et al.*, 2004], NOAA-11 SBUV/2 [*DeLand and Cebula*, 1998], Global Ozone Monitoring Experiment (GOME) [*Weber et al.*, 1998], Scanning Imaging Absorption spectroMeter for Atmospheric CHartographY (SCIAMACHY) [*Pagaran et al.*, 2009], Solar Radiation and Climate Experiment (SORCE) Spectral Irradiance Monitor (SIM) [*Harder et al.*, 2009], and SORCE SOLSTICE [*Snow et al.*, 2010]. Analysis of solar UV irradiance data is complicated by the degradation of satellite instrument response, which may have a complex spectral and temporal dependence [e.g., *Floyd et al.*, 1998; *DeLand and Cebula*, 2008].

[4] *Heath and Schlesinger* [1986] first developed the Mg II core-to-wing index as a solar activity proxy that could overcome these difficulties. The Mg II index is generally defined as the ratio of the chromospheric emission from the *h* and *k* lines at 280 nm to the photospheric flux at approximately 277 and 283 nm in the wings of the feature. This ratio cancels out most of the time-dependent degradation effects in

[1]Science Systems and Applications, Inc., Lanham, Maryland, USA.

Corresponding author: M. DeLand, Science Systems and Applications, Inc., 10210 Greenbelt Road, Suite 600, Lanham, MD 20706, USA. (matthew.deland@ssaihq.com)

2169-897X/13/10.1002/jgrd.50310

the irradiance data, and the use of wing irradiances equally spaced about the core irradiance cancels out any spectrally dependent degradation that can be characterized as linear over this short wavelength interval. The Mg II index has proven to be a robust and valuable measure of solar UV activity, and data sets from many instruments are now available [e.g., *Cebula and DeLand*, 1998; *Weber et al*., 1998; *Floyd et al*., 2003; *Snow et al*., 2005]. Good agreement between the Mg II index and Ca II K indexes derived from ground-based images has been shown by numerous authors [e.g., *Kariyappa and Pap*, 1996; *Bertello et al*., 2010; *Morrill et al*., 2011a]. In addition, relationships between short-term variations have been used to parameterize the Mg II index to estimate irradiance variations at other UV wavelengths [*Heath and Schlesinger*, 1986; *DeLand and Cebula*, 1993; *Pagaran et al*., 2009].

[5] It would be useful to have comparable indicators of solar activity from satellite measurements to represent other parts of the UV spectrum, particularly longward of ~290 nm where long-term solar variations decrease significantly in amplitude. While the Ca II K and H features are comparable in overall depth to the Mg II feature, the magnitude of the "core" irradiance variation is substantially smaller (approximately a factor of 4). Thus, the ability to construct a useful Ca II core-to-wing index is more dependent on satellite instrument performance parameters such as signal-to-noise ratio, stray light rejection, nonlinearity, and wavelength scale drift. For example, *Weber et al*. [1998] were only able to show direct Ca II K irradiance values from GOME measurements because of the relatively high noise levels observed in the wings of the feature. In this paper, we present Ca II K, Ca II H, and Mg II index data sets derived from measurements made by the Ozone Monitoring Instrument (OMI) flying on the Aura spacecraft since July 2004. The excellent long-term performance of OMI allows us to create daily data sets of Ca II H, Ca II K, and Mg II index values (with only one data gap in 2006) that agree very well with each other and with concurrent Mg II index data sets from other satellite instruments. We have also created a similar index using the Mg I feature at 285.2 nm. The OMI Ca II K index data also provide an opportunity to validate the Ca II K index data derived from Integrated Sunlight Spectrometer (ISS) measurements at the National Solar Observatory (NSO) since 2006. This comparison shows the presence of some anomalous data points in the ground-based NSO data set and further demonstrates the value of solar UV spectral irradiance measurements from satellites.

2. OMI Instrument

[6] OMI is a single monochromator that covers the wavelength range 264–504 nm using three separate detectors with overlapping spectral coverage. The detectors are identified as UV-1 (wavelength range = 264–311 nm, resolution $\Delta\lambda = 0.63$ nm), UV-2 (range = 307–383 nm, $\Delta\lambda = 0.42$ nm), and VIS (range = 349–504 nm, $\Delta\lambda = 0.63$ nm). Additional instrument details are discussed in *Levelt et al*. [2006]. The primary purpose of OMI is the measurement of ozone and other trace gases using backscattered radiation. OMI uses a 2-D charge-coupled device to view the Earth in the nadir, with 60 spatial rows in the cross-track direction and wavelength oriented in the along-track direction. Each pair of adjacent spatial rows is combined in UV-1 data to improve signal-to-noise performance. Daily solar measurements, intended primarily for instrument calibration, are made by viewing the Sun through a special port with a set of diffusers. Figure 1 shows an example of the solar irradiance spectrum measured by OMI. All spatial rows collect data simultaneously in this operating mode, so that either 30 spectra (UV-1 detector) or 60 spectra (VIS detector) can be combined for each measurement. The nominal integration time for solar measurements is 2 s, which allows up to 77 data frames to be collected and eventually averaged during each solar observation. This approach results in excellent signal-to-noise ratios for the irradiance data used to create the proxy indexes.

[7] Overall, OMI has shown remarkable long-term radiometric stability during its mission. In-orbit measurements demonstrate approximately linear degradation trends for all three detectors. *Dobber et al*. [2008] show changes of approximately 1.2% in the UV-1 detector and 0.5% in the UV-2 and VIS detectors during the first 2.5 years of operation, and these degradation rates have continued throughout the mission. Monitoring of spectral features in the UV-2 detector shows that any systematic instrumental wavelength shifts do not exceed 0.005 nm over the 8-year lifetime of the instrument. However, when assessing the relatively low level of the chromospheric

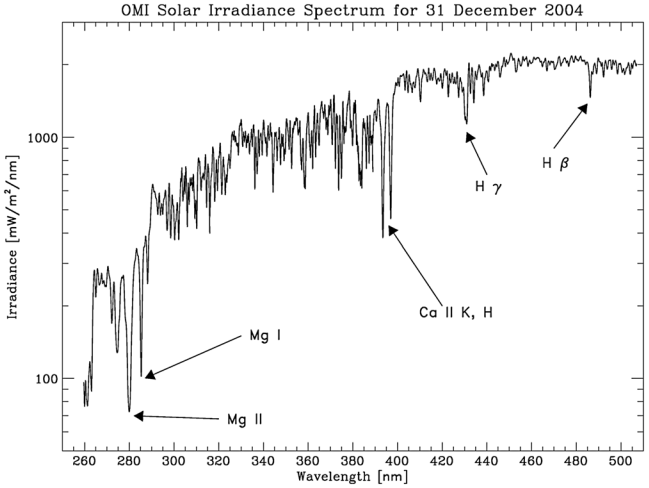

Figure 1. The OMI solar irradiance spectrum measured on 31 December 2004.

variability in the Mg II and Ca II features, we must consider the possibility of additional small amplitude systematic errors in the solar indices stemming from incompletely characterized instrumental trends. In order to lessen the impact of such errors, we have compared our Mg II index data to all publicly available time series. We find that the overall agreement between these data sets can be improved by introducing two separate multiplicative adjustments. The first adjustment is a periodic term that removes annual variations associated with solar goniometry, i.e., the changes in the Sun's azimuth and elevation angle on the solar diffuser. The amplitude of this correction is ~0.1% peak to valley for the Mg II index based on UV-1 data (Figure 2a), increasing to ~1% for the Ca II index based on VIS data. Separately, we have observed that the depth of Fraunhofer lines in the UV-2 spectral region has increased by 0.2–0.3% during the 8 years of OMI operation. We attribute this instrumental trend to a gradual change in OMI stray light characteristics. Detailed modeling shows that the current version of the Ground Data Processing Software (see *Dobber et al*. [2008] and references therein) slightly underestimates the stray light component in the UV-2 detector. To correct similar instrumental drifts in the UV-1 and VIS detectors, we calculated a long-term linear adjustment of approximately 0.4% for the OMI Mg II index data (Figure 2b) and a comparable adjustment of approximately 0.3% for the Ca II index data. We discuss these adjusted OMI data sets in the following sections.

3. OMI Mg and Ca Chromospheric Indices

[8] The spectral resolution of OMI does not allow separation of the emission peaks at the cores of the Ca II H, Ca II K lines, and the Mg II doublet. We therefore construct OMI solar indexes using the "traditional" approach, i.e., calculating the ratio of the core irradiance (as a mean flux in the given wavelength interval) to the average of the wing irradiances:

$$\mathrm{Mg\,II} = 2^{*}F(280.0\,\mathrm{nm})/[F(277.0\,\mathrm{nm}) + F(283.0\,\mathrm{nm})] \quad (1)$$

$$\mathrm{Ca\,II\,K} = 2^{*}F(393.5\,\mathrm{nm})/[F(390.1\,\mathrm{nm}) + F(400.1\,\mathrm{nm})] \quad (2)$$

$$\mathrm{Ca\,II\,H} = 2^{*}F(397.0\,\mathrm{nm})/[F(390.1\,\mathrm{nm}) + F(400.1\,\mathrm{nm})] \quad (3)$$

[9] Note that, in order to increase the signal-to-noise ratio and partially overcome some wavelength sampling limitations, we average the core irradiance for the Mg II index over 279.7–280.2 nm, while irradiances in the wings of the feature are averaged over 276.8–277.1 nm and 282.9–283.2 nm, respectively. For the Ca II K and H indexes, the irradiances in the line wings are averaged over 389.1–391.1 nm and 399.1–401.1 nm to ensure the best representation of the pseudocontinuum irradiance. The core irradiance values are then estimated at the precise wavelengths of each emission feature, 393.48 and 396.96 nm, respectively, after combining all available solar spectra (up to 60 in this wavelength range) for each measurement. This procedure improves the accuracy of the Ca II core irradiance values.

[10] We first discuss the OMI Mg II index data in order to establish its agreement and overall consistency with other concurrent observations. The time series of this data set from September 2004 to July 2012 is shown in Figure 3. The absolute value of the Mg II index observed by two (or more) satellite instruments can differ as a result of the spectral resolution of each instrument and the exact choice of wavelengths used to calculate the index, as shown by *Viereck et al*. [2004]. Previous work by *de Toma et al*. [1997] and *White et al*. [1998] demonstrated that Mg II indexes derived from SBUV/2 and UARS SOLSTICE measurements with different spectral resolutions could be adjusted to a common scale using simple linear relationships. We therefore followed the same approach and transformed overlapping data sets from multiple instruments to the OMI reference scale for further comparison. Table 1 lists the regression coefficients for these transformations, which all have very high correlation coefficients of 0.95 or better.

[11] The short-term agreement between the individual Mg II index data sets is excellent, as shown by the daily values for three consecutive solar rotations in mid-2005 (Figure 4). We can examine time series of the ratio between these scaled data sets and the OMI Mg II index for evidence of residual instrumental trends. For example, Figure 5 shows that the SCIAMACHY Mg II data set drifts by approximately +0.5% relative to OMI during 2004–2008, then drops abruptly in late 2008, possibly due to a decontamination heating event [see *Pagaran et al*., 2009]. The ratio values in this figure have been binned in 30 day averages for clarity. Figure 6 shows similar comparisons with the NOAA-16, NOAA-17, and NOAA-18 Mg II index data sets. The

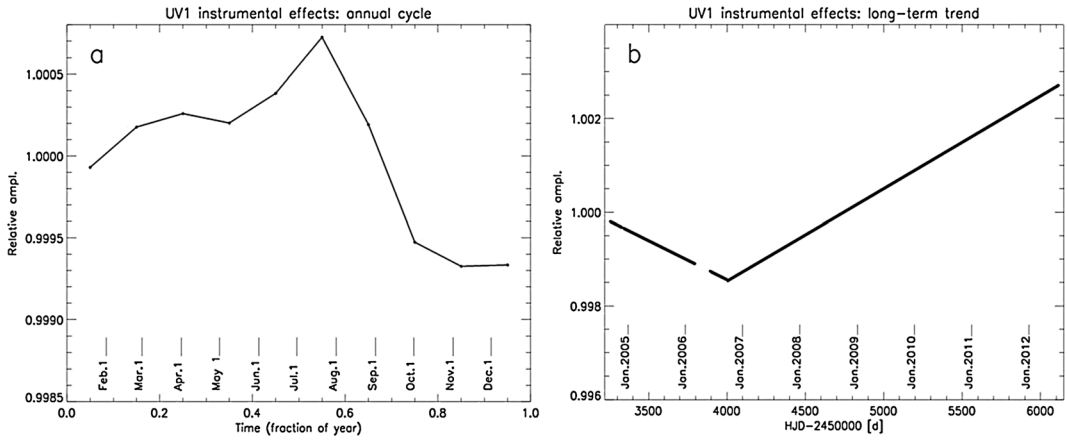

Figure 2. Adjustments for instrument behavior applied to the OMI Mg II index data set. (a) Periodic annual variation. (b) Long-term trend. Time is given in heliocentric Julian days (HJD)—2450000.0.

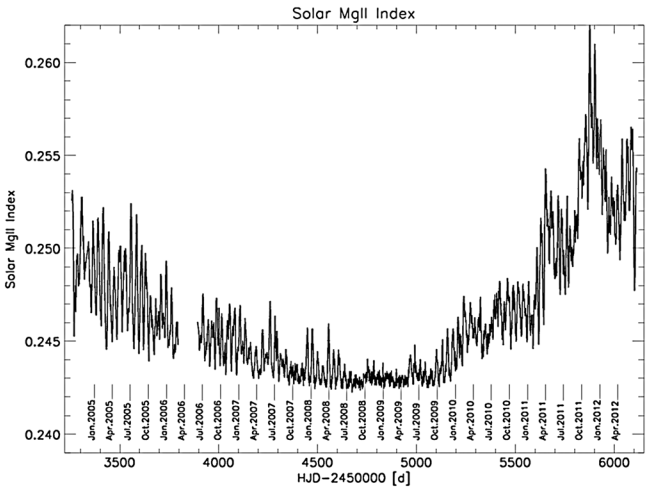

Figure 3. The daily Mg II index observed by Aura OMI. Note that no OMI solar data are available from 27 February 2006 to 16 June 2006.

NOAA-16 ratio with OMI shows no drift to within 0.4%, which represents the scatter of the ratio data points. The NOAA-17 and NOAA-18 time series both show a few tenths of a percent drift relative to OMI through late 2008, but then the NOAA-17 data show a more rapid decrease of 0.4–0.6% after that time. We currently believe that this represents an uncorrected calibration error in the NOAA-17 SBUV/2 data set. Figure 7 shows the ratio comparison between the OMI and SORCE SOLSTICE Mg II index data sets. This ratio shows no long-term drift. The day-to-day scatter in these ratio values is approximately 0.5% peak to peak, consistent with other comparisons between different Mg II index data sets.

[12] The Mg I absorption feature at 285.2 nm is also quite deep but is considerably narrower than the Mg II feature. This increases the difficulty of deriving useful solar activity index values from moderate-resolution OMI irradiance data. Nevertheless, we have also produced a useful OMI Mg I index data set by averaging the core irradiance for the Mg I index over 285.0–285.5 nm. The irradiances in the wings of the feature are averaged over 282.9–283.2 nm and 286.7–287.4 nm, respectively.

$$\mathrm{Mg\,I} = 2^{*}F(285.2\,\mathrm{nm})/[F(283.0\,\mathrm{nm}) + F(287.0\,\mathrm{nm})] \quad (4)$$

[13] Figure 8 shows the OMI Mg I and Mg II index values during the rising portion of cycle 24. While the Mg I index time series does exhibit more anomalous single-day spikes, which are unlikely to represent true UV irradiance variations, rotational modulations as small as 0.5% peak to peak are consistently observed in both data sets. We have also calculated core-to-wing index values for the prominent H-γ (434.08 nm) and H-β (486.13 nm) absorption features in the visible range. We find that the derived index values for these features are dominated by instrument noise so that an upper limit for solar cycle variability observed by OMI in these lines is 0.5%.

4. Comparison of the OMI Ca II K Index to Various Solar Activity Indicators

[14] The OMI Ca II K index time series is shown in Figure 9, along with the OMI Mg II data scaled to the Ca II K measurements and offset by +0.005 for clarity. The Ca II K index clearly follows the same solar cycle variation as the Mg II index, with an overall correlation coefficient of $R_{\mathrm{Ca\ II\ K}} = 0.98$ (see Table 2), and well-resolved solar rotational modulations visible throughout 2005. The OMI Ca II H index also has a correlation coefficient of $R_{\mathrm{Ca\ II\ H}} = 0.98$ with the OMI Mg II index. The weaker amplitude of the chromospheric variability in the Ca II K line becomes more evident during cycles 23–24 minimum in 2008–2009. The period between January–April 2009 has essentially no rotational modulation, so any variability should represent day-to-day noise and scatter. The ±1 σ variability of the OMI Ca II K index during this time is approximately four times larger than the OMI Mg II index when both data sets are normalized to their average values.

[15] Figure 10 shows scatterplot comparisons of OMI solar proxy indexes with other indicators of solar UV activity.

Table 1. The Linear Transformation Coefficients for the OMI Mg II Solar Index, as Derived From $\mathrm{MgII_{OMI}} = A_0 + A_1 * \mathrm{MgII}_X$[a]

Mission	A_0	A_1	Corr	Data Set Location
GOME	0.109	1.007	0.953	http://www.iup.uni-bremen.de/gome/solar/GOME_Index_integrate.dat
SCIAMACHY	0.064	1.189	0.984	http://www.iup.uni-bremen.de/gome/solar/SCIA_index_integrate.dat
SORCE SOLSTICE	0.199	0.808	0.989	http://lasp.colorado.edu/sorce/ssi_data/mgii/txt/sorce_mg_latest.txt
NOAA-16 SBUV/2	−0.042	1.100	0.990	http://sbuv2.gsfc.nasa.gov/solar/mgii/noaa16_mgii_fill_20111031.txt
NOAA-17 SBUV/2	−0.015	1.009	0.966	http://sbuv2.gsfc.nasa.gov/solar/mgii/noaa17_mgii_fill_20110905.txt
NOAA-18 SBUV/2	−0.057	1.158	0.988	http://sbuv2.gsfc.nasa.gov/solar/mgii/noaa18_mgii_fill_20111031.txt

[a]The correlation coefficient is also listed.

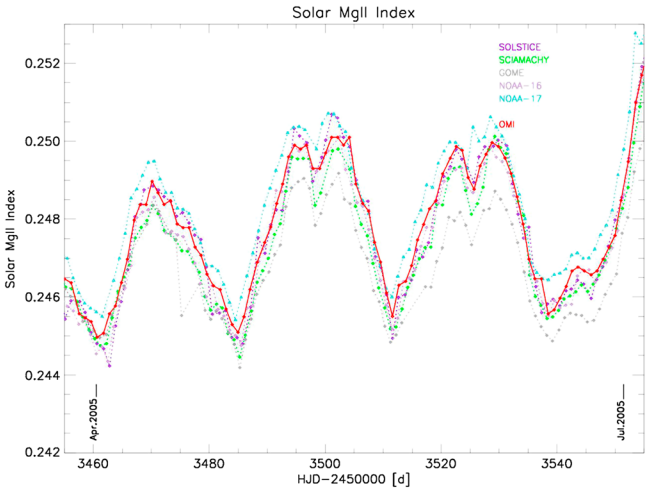

Figure 4. Solar rotational modulation in 2005 as observed in Mg II index data from multiple satellite instruments. All data sets have been adjusted to the OMI reference level. Note the consistent representation of the small dips with amplitudes <0.5% between days 3495–3500 and 3520–3530, as well as the local ~0.2% maximum around day 3543.

Linear regression results for these comparisons are also listed in Table 2. The excellent agreement between the OMI Ca II and Mg II indexes can be seen in Figure 10a, while Figure 10b shows almost perfect agreement between the OMI Mg II and SORCE SOLSTICE Mg II data ($R_{\mathrm{SOLSTICE}} = 0.99$). The slight deviation from linearity at the bottom left of this panel suggests that the higher-resolution SORCE measurement continues to detect variations near solar minimum that are not represented in the lower-resolution OMI measurements. These points correspond to the lowest values in Figure 7 between days 4300 and 5000. The OMI Ca II data also closely follow the SORCE SOLSTICE Mg II index, albeit with slightly more scatter (Figure 10c).

[16] The NOAA-17 and NOAA-18 SBUV/2 instruments have an electronics change compared to previous SBUV/2 instruments that improves their signal-to-noise characteristics and thus allows derivation of useful Ca II K index values from daily continuous scan irradiance measurements. These measurements are made with an instrument resolution of 1.1 nm and only collect two samples per day, so we expect more noise in the SBUV/2 Ca II K index values relative to OMI data. Figure 10d shows that the overall comparison is still quite good ($R_{\mathrm{NOAA\text{-}18}} = 0.93$), with a lower correlation coefficient for NOAA-17 Ca II K data ($R_{\mathrm{NOAA\text{-}17}} = 0.85$) weighted by low NOAA-17 values related to certain instrument operations.

[17] In order to compare the OMI Mg II index data and the 10.7 cm flux measured at Penticton, we first scaled both data sets by their mean values before linearly transforming the normalized radio flux into the OMI frame of reference. These regression coefficients are not included in Table 2. This comparison produces a lower correlation coefficient ($R_{10.7} = 0.84$), which is caused by numerous short-term

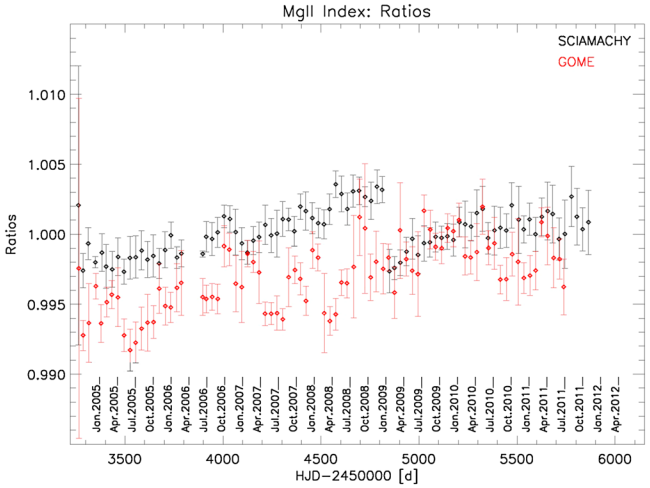

Figure 5. Ratio of SCIAMACHY and GOME Mg II index daily values to OMI Mg II index daily values, binned in 30 day averages. The error bars represent the ±1 σ standard deviation of individual values in each 30 day bin.

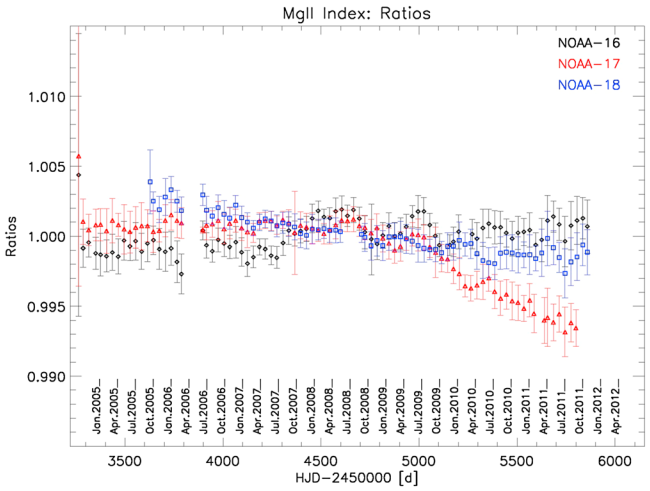

Figure 6. Ratios of NOAA-16, NOAA-17, and NOAA-18 SBUV/2 Mg II index daily values to OMI Mg II index daily values, binned in 30 day averages. NOAA-16 Mg II index data have been excluded in late 2009 and early 2010 due to measurement errors caused by orbit drift. NOAA-17 Mg II index data have been excluded after September 2011 due to measurement errors caused by orbit drift. NOAA-18 Mg II index data are not available from 23 May 2008 to 25 August 2008.

bursts in 10.7 cm flux during periods of high solar activity that are not fully reflected in the Mg II index data. The Mg II index is a more effective proxy for short-term chromospheric variations [e.g., *Viereck et al*., 2001], whereas 10.7 cm flux gives a better representation of coronal activity. Figure 10e shows a slight change in the scatterplot slope for these high-activity events.

[18] Figure 10f shows a comparison between the OMI Ca II K index data and the NSO Ca II K index data set derived from ISS measurements using a 1.0 Å band pass [*Bertello et al*., 2011]. While these two data sets are clearly well correlated, there are some anomalously high data points observed in the NSO 1.0 Å data set that are not present in the corresponding OMI data. These elevated NSO Ca II K index values are evident in the time series plot shown in Figure 11. Similar elevated data points are present in the NSO Ca II H data set, although with different magnitudes and not always on the same dates. No corresponding anomalous values are seen in the concurrent NOAA-18 Ca II K index, OMI Mg II index, or SORCE Mg II index data sets. We thus believe that these points represent problems with the NSO ISS measurements or data processing. The excellent stability and daily cadence of the OMI solar measurements, with no interruptions due to surface weather, makes it useful for validation and screening of the NSO measurements.

[19] In contrast to our OMI results shown in Figures 10a and 10c, *Morrill et al*. [2011b] found a slightly nonlinear relationship between NOAA composite Mg II index values during 1991–1995 and Ca II disk activity determined from Big Bear Solar Observatory (BBSO) images. We note that the OMI Ca II K index represents a disk-integrated measure of irradiance variations, whereas the BBSO Ca II K values (determined as fraction of the solar disk with enhanced activity due to plages, network, or sunspots) represent the areal extent of enhanced activity without further quantifying the magnitude of the enhancement. Thus, a single numerical value for the area of enhanced activity may correspond to

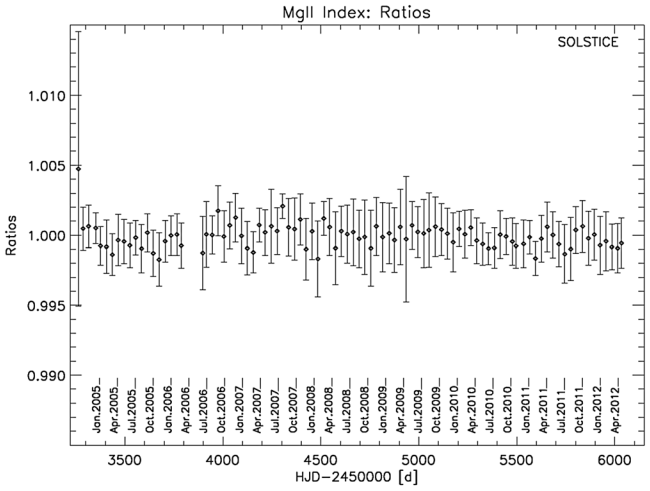

Figure 7. Ratio of SORCE SOLSTICE Mg II index daily values to OMI Mg II index daily values, binned in 30 day averages.

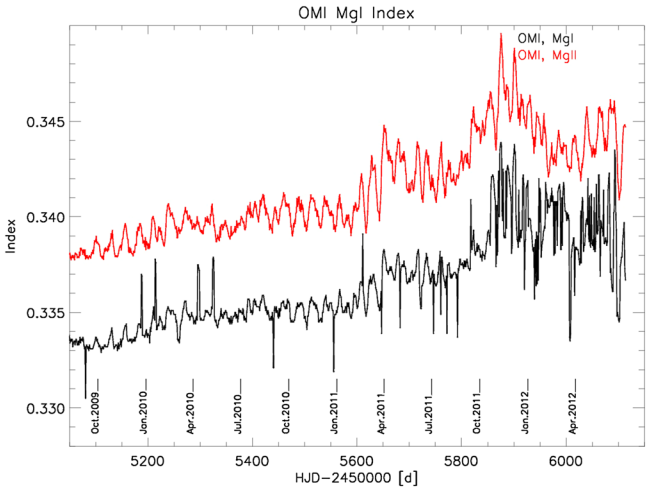

Figure 8. OMI Mg II and Mg I index data sets during the rising portion of cycle 24. The Mg II index data have been scaled to the Mg I reference level and shifted by +0.005 for clarity.

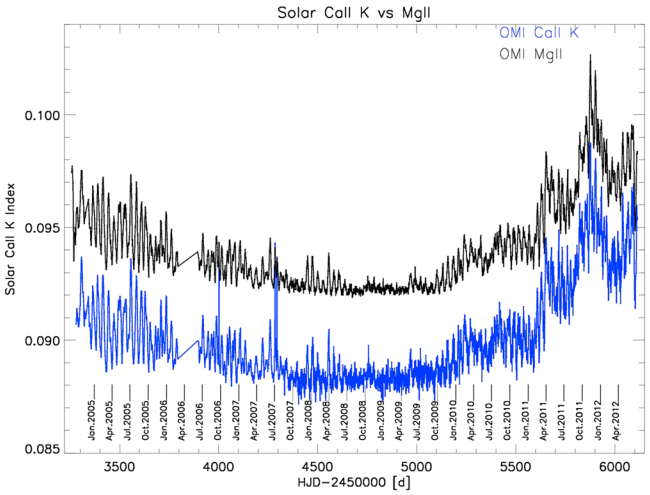

Figure 9. OMI Ca II K and Mg II indexes. The Mg II and Ca II K indexes have been scaled to the NSO Ca II K index reference level. The scaled Mg II index has been offset by +0.005 for clarity.

different levels of increased irradiance on different occasions. This is demonstrated by the larger scatter of Mg II index values for higher levels of solar activity in Figure 14 of *Morrill et al*. [2011b], whereas the scatter between OMI Ca II K and Mg II index values in Figure 10a remains constant for all levels of solar activity (see also the SORCE SOLSTICE comparison in Figure 10c). Although the third-order function relating Mg II index values to Ca II K activity derived by *Morrill et al*. [2011b] does not depart significantly from a linear dependence, users should be aware that there is a difference from the relationship derived in this paper.

Table 2. Linear Regression Fit Parameters Between Different Solar Activity Indices Shown in This Paper, as Derived From $Y = A_0 + A_1 * X$[a]

X Data Set	*Y* Data Set	A_0	A_1	Corr
OMI Mg II	OMI Mg I	−0.314	1.671	0.831
NSO Ca II K	OMI Ca II K	−0.513	4.180	0.918
NSO Ca II H	OMI Ca II H	−0.476	3.594	0.939
OMI Mg II	OMI Ca II K	−0.779	7.114	0.978
OMI Mg II	OMI Ca II H	−1.153	8.892	0.977
SORCE SOLSTICE Mg II	OMI Ca II K	−1.187	8.644	0.970
SORCE SOLSTICE Mg II	OMI Ca II H	−1.630	10.74	0.968
NOAA-17 SBUV/2 Ca II K	OMI Ca II K	0.235	1.357	0.854
NOAA-18 SBUV/2 Ca II K	OMI Ca II K	0.199	1.621	0.927

[a]The correlation coefficient is also listed.

5. Conclusion

[20] Many satellite instruments designed for terrestrial remote sensing using backscattered UV radiation have proven to be valuable monitors of solar activity. We have shown that the OMI instrument on Aura continues this capability, producing an Mg II core-to-wing index that is equal in quality to the best currently available Mg II data set from SORCE SOLSTICE. The excellent performance and spectral coverage of the OMI instrument also allow the derivation of a Ca II K core-to-wing ratio data set, despite the lower level of activity in this solar feature. The OMI Ca II K index agrees very well

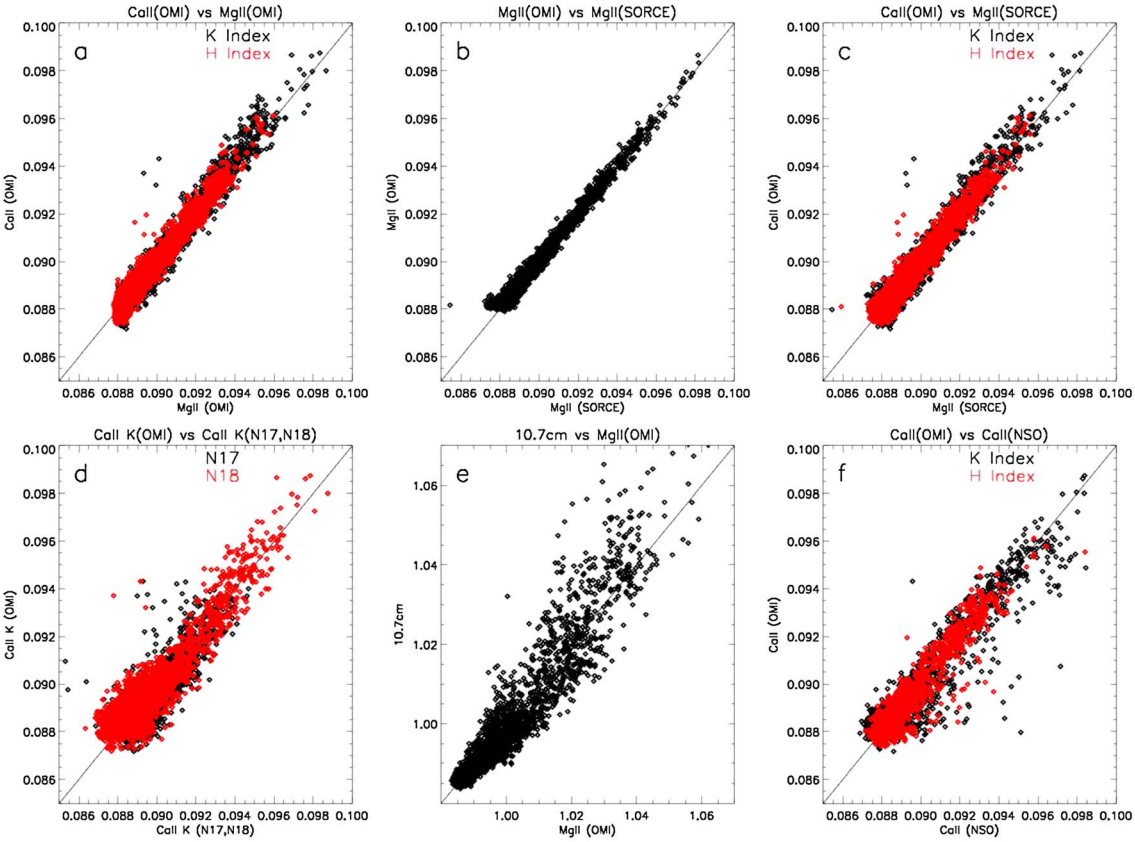

Figure 10. Scatterplot comparisons between different solar activity indexes. In all panels, the *Y*-axis data set has been scaled to the *X*-axis data set to illustrate the linearity of the comparison using the transformations listed in Table 2. (a) OMI Ca II K and H indexes versus OMI Mg II index. (b) OMI Mg II index versus SORCE SOLSTICE Mg II index. (c) OMI Ca II K and H indexes versus SORCE SOLSTICE Mg II index. (d) OMI Ca II K indexes versus NOAA-17 and NOAA-18 Ca II K indexes. (e) Penticton 10.7 cm flux (normalized) versus OMI Mg II index (normalized). (f) OMI Ca II K and H indexes versus NSO Ca II K 1.0 Å index.

with the OMI Mg II index over 8 years of measurements, confirming relationships previously predicted on the basis of short-term variations alone. The daily cadence and high quality of the OMI Ca II K index also makes it possible to identify anomalous values in ground-based NSO Ca II data sets. The OMI Mg II and Ca II index values are currently available online at http://sbuv2.gsfc.nasa.gov/solar/omi/, and eventually will be updated on a daily basis by the NASA Team Leader Computing

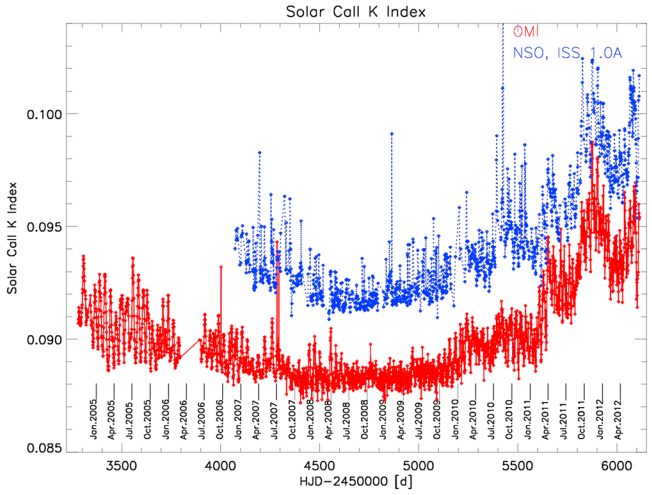

Figure 11. NSO Ca II K 1.0 Å index and OMI Ca II K data scaled to the NSO reference level. The NSO data have been shifted by +0.004 for clarity.

Facility system that processes all OMI data products. OMI solar measurements are expected to continue as solar activity rises toward the peak of cycle 24, and a successor instrument (TROPOMI) that emphasizes tropospheric remote sensing is scheduled to launch on the ESA/GMES Sentinel 5 Precursor mission in late 2014. We therefore expect to continue producing our Mg II and Ca II K index data sets well into the future.

[21] **Acknowledgments.** Support for processing and analysis of OMI data was provided by NASA contract NNG06HX18C. We are thankful to L. Flynn for numerous suggestions that helped to improve the content of this paper. We appreciate the useful comments provided by three anonymous reviewers. This study used solar radio 10.7 cm flux data from the Penticton Dominion Radio Astrophysical Observatory (NRC of Canada).

References

Bertello, L., R. K. Ulrich, and J. E. Boyden (2010), The Mount Wilson Ca II K plage index time series, *Sol. Phys.*, *264*, 31–44.

Bertello, L., A. A. Pevtsov, J. W. Harvey, and R. W. Toussaint (2011), Improvements in the determination of ISS Ca II K parameters, *Sol. Phys.*, *272*, 229–245.

Brasseur, G. P., and S. Solomon (2005), Aeronomy of the Middle Atmosphere: Chemistry and Physics of the Stratosphere and Mesosphere, 3rd ed., 644 pp., Springer, Berlin.

Cebula, R. P., and M. T. DeLand (1998), Comparison of the NOAA-11 SBUV/2, UARS SOLSTICE, and UARS SUSIM Mg II solar activity proxy indexes, *Sol. Phys.*, *177*, 117–132.

DeLand, M. T., and R. P. Cebula (1993), Composite Mg II solar activity index for solar cycles 21 and 22, *J. Geophys. Res.*, *98*, 12,809–12,823.

DeLand, M. T., and R. P. Cebula (1998), NOAA 11 Solar Backscattered Ultraviolet, model 2 (SBUV/2) instrument solar spectral irradiance measurements in 1989–1994: 2. Results, validation, and comparison, *J. Geophys. Res.*, *103*, 16,251–16,273.

DeLand, M. T., and R. P. Cebula (2001), Spectral solar ultraviolet irradiance data for cycle 21, *J. Geophys. Res.*, *106*, 21,569–21,583.

DeLand, M. T., and R. P. Cebula (2008), Creation of a composite solar ultraviolet irradiance data set, *J. Geophys. Res.*, *113*, A11103, doi:10.1029/2008JA013401.

DeLand, M. T., R. P. Cebula, and E. Hilsenrath (2004), Observations of solar spectral ultraviolet irradiance change during cycle 22 from NOAA-9 Solar Backscattered Ultraviolet Model 2 (SBUV/2), *J. Geophys. Res.*, *109*, D06304, doi:10.1029/2003JD004074.

Dobber, M., Q. Kleipool, R. Dirksen, P. Levelt, G. Jaross, S. Taylor, T. Kelly, L. Flynn, G. Leppelmeier, and G. Rozemeijer (2008), Validation of ozone monitoring instrument level 1b data products, *J. Geophys. Res.*, *113*, D15S06, doi:10.1029/2007JD008665.

Ermolli, I., S. K. Solanki, A. G. Tlatov, N. A. Krivova, R. K. Ulrich, and J. Singh (2009), Comparison among Ca II K spectroheliogram time series with an application to solar activity studies, *Astrophys. J.*, *698*, 1000–1009.

Floyd, L. E., L. C. Herring, D. K. Prinz, and P. C. Crane (1998), Instrument responsivity evolution of SUSIM UARS, *Proc. SPIE*, *3427*, 445–456.

Floyd, L. E., J. W. Cook, L. C. Herring, and P. C. Crane (2003), SUSIM's 11-year observational record of the solar ultraviolet irradiance, *Adv. Space Res.*, *31*, 2111–2120.

Foukal, P., L. Bertello, W. C. Livingston, A. A. Pevtsov, J. Singh, A. G. Tlatov, and R. G. Ulrich (2009), A century of solar Ca II measurements and their implication for solar UV driving of climate, *Sol. Phys.*, *255*, 229–238.

Harder, J. W., J. M. Fontenla, P. Pilewskie, E. C. Richard, and T. N. Woods (2009), Trends in solar spectral irradiance variability in the visible and infrared, *Geophys. Res. Lett.*, *36*, L07801, doi:10.1029/2008GL036797.

Heath, D. F., and B. M. Schlesinger (1986), The Mg 280-nm doublet as a monitor of changes in solar ultraviolet irradiance, *J. Geophys. Res.*, *91*, 8672–8682.

Kariyappa, R., and J. Pap (1996), Contributions of chromospheric features to UV irradiance variability from spatially resolved Ca II K spectroheliograms. I. A new method of analysis and preliminary results, *Sol. Phys.*, *167*, 115–123.

Keil, S. L., and S. P. Worden (1984), Variations in the solar calcium K line 1976-1982, *Astrophys. J.*, *276*, 766–781.

Lean, J. L., G. J. Rottman, H. L. Kyle, T. N. Woods, J. R. Hickey, and L. C. Puga (1997), Detection and parameterization of variations in solar mid- and near-ultraviolet radiation (200-400 nm), *J. Geophys. Res.*, *102*, 29,939–29,956.

Levelt, P. F., G. H. J. van den Oord, M. R. Dobber, A. Mälkki, H. Visser, J. de Vries, P. Stammes, J. O. V. Lundell, and H. Saari (2006), The ozone monitoring instrument, *IEEE Geosci. Trans. Rem. Sens.*, *44*, 1093–1101.

Livingston, W., O. R. White, L. Wallace, and J. Harvey (2010), Sun-as-a-star, chromospheric lines, 1974-2009, *Mem. Soc. Astron. Ital.*, *81*, 643–645.

Morrill, J. S., L. Floyd, R. Ulrich, S. Weaver, and D. McMullin (2011a), Estimating the Mg II index from 1961 through 1981 using Ca II K images from the Mt. Wilson Observatory, *Sol. Phys.*, *270*, 109–124.

Morrill, J. S., L. Floyd, and D. McMullin (2011b), The solar ultraviolet spectrum estimated using the Mg II index and Ca II K disk activity, *Sol. Phys.*, *269*, 253–267.

Pagaran, J., M. Weber, and J. Burrows (2009), Solar variability from 240 to 1750 nm in terms of faculae brightening and sunspot darkening from SCIAMACHY, *Astrophys. J.*, *700*, 1884–1895.

Rottman, G. J. (1988), Observations of solar UV and EUV variability, *Adv. Space Res.*, *8*(7), 53–66.

Rottman, G., T. Woods, M. Snow, and G. de Toma (2001), The solar-cycle variation in ultraviolet irradiance, *Adv. Space Res.*, *27*, 1927–1932.

Snow, M., W. E. McClintock, T. N. Woods, O. R. White, J. W. Harder, and G. Rottman (2005), The Mg II index from SORCE, *Sol. Phys.*, *230*, 325–344.

Snow, M., W. E. McClintock, and T. N. Woods 2010, Solar spectral irradiance variability in the ultraviolet from SORCE and UARS SOLSTICE, *Adv. Space Res.*, *46*, 296-302.

Tlatov, A. G., A. A. Pevtsov, and J. Singh (2009), A new method of calibration of photographic plates from three historic data sets, *Sol. Phys.*, *255*, 239–251.

de Toma, G., O. R. White, B. G. Knapp, G. J. Rottman, and T. N. Woods (1997), Mg II core-to-wing index: Comparison of SBUV2 and SOLSTICE time series, *J. Geophys. Res.*, *102*, 2597–2610.

Viereck, R., L. Puga, D. McMullin, D. Judge, M. Weber, and W. K. Tobiska (2001), The Mg II index: A proxy for solar EUV, *Geophys. Res. Lett.*, *28*, 1343–1346.

Viereck, R. A., L. E. Floyd, P. C. Crane, T. N. Woods, B. G. Knapp, G. Rottman, M. Weber, L. C. Puga, and M. T. DeLand (2004), A composite Mg II index spanning from 1978 to 2003, *Space Weather*, *2*, S10005, doi:10.1029/2004SW000084.

Weber, M., J. P. Burrows, and R. P. Cebula (1998), GOME solar irradiance measurements between 1995 and 1997: First results on proxy solar activity studies, *Sol. Phys.*, *177*, 63–77.

White, O. R., and W. C. Livingston (1981), Solar luminosity variation. III—Calcium K variations from solar minimum to maximum in cycle 21, *Astrophys. J.*, *249*, 798–816.

White, O. R., G. de Toma, G. J. Rottman, T. N. Woods, and B. G. Knapp (1998), Effect of spectral resolution on the Mg II index as a measure of solar variability, *Sol. Phys.*, *177*, 89–103.